2014

Enhanced magnetic anisotropy in cobalt-carbide nanoparticles

Ahmed A. El-Gendy
Virginia Commonwealth University, aelgendy@vcu.edu

Meichun Qian
Virginia Commonwealth University, mqian@vcu.edu

Zachary J. Huba
Virginia Commonwealth University

Shiv N. Khanna
Virginia Commonwealth University, snkhanna@vcu.edu

Everett E. Carpenter
Virginia Commonwealth University, ecarpenter2@vcu.edu

El-Gendy, A.A., Qian, M., Huba, Z.J., et al., Enhanced magnetic anisotropy in colbalt-carbide nanoparticles. Applied Physics Letters, 104, 023111 (2014).

Enhanced magnetic anisotropy in cobalt-carbide nanoparticles

Ahmed A. El-Gendy,[1,2,a)] Meichun Qian,[3] Zachary J. Huba,[1] Shiv N. Khanna,[3,a)] and Everett E. Carpenter[1,a)]
[1]*Department of Chemistry, Virginia Commonwealth University, Virginia 23284, USA*
[2]*Nanotechnology and Nanometrology laboratory, National institute for standards, Giza 12211, Egypt*
[3]*Department of Physics, Virginia Commonwealth University, Virginia 23284, USA*

(Received 1 August 2013; accepted 28 December 2013; published online 15 January 2014)

An outstanding problem in nano-magnetism is to stabilize the magnetic order in nanoparticles at room temperatures. For ordinary ferromagnetic materials, reduction in size leads to a decrease in the magnetic anisotropy resulting in superparamagnetic relaxations at nanoscopic sizes. In this work, we demonstrate that using wet chemical synthesis, it is possible to stabilize cobalt carbide nanoparticles which have blocking temperatures exceeding 570 K even for particles with magnetic domains of 8 nm. First principles theoretical investigations show that the observed behavior is rooted in the giant magnetocrystalline anisotropies due to controlled mixing between C *p*- and Co *d*-states. © *2014 AIP Publishing LLC*. [http://dx.doi.org/10.1063/1.4862260]

Magnetic nanoparticles are key to the high-density memory storage, targeted drug delivery, and a variety of other industrial and medical applications, including components in nano-electronic circuits.[1–6] Starting from the bulk magnetic material, the decrease in size smaller than the typical domain size results in a nanomagnet where the atomic moments are exchange coupled. This causes the particle to behave like a giant magnet with a moment $N\mu$, where N is the number of atoms while μ is the moment per atom. In the ultrafine particles, however, the magnetic anisotropy energy responsible for holding the magnetic moment along certain directions becomes comparable to the thermal energy.[7,8] This allows for thermal fluctuations which produce random flipping of the magnetic moment with time leading to thermal instability of the magnetization. The key to thermally stable magnetic nanoparticles is then to enhance the anisotropy. One approach proposed recently by Skumryev *et al.*[9,10] is to generate core shell species where the central metallic core is surrounded by an oxide material that can enhance anisotropy through exchange bias. These authors synthesized Co/CoO nanoparticles with exchange bias between the central ferromagnet and the surrounding antiferromagnetic oxide. The particles have blocking temperatures of around 290 K close to room temperature. Another approach has been suggested, as well, to generate core/shell nanoalloys. In that approach, the authors introduced an enhanced magnetocrystalline anisotropy in the range of 0.3 to 2.6 $\times$ 10^5 J/m^3 for 8 nm NiRu@C nanoalloy.[11] However, the T_B was in range from 50 to 200 K which is below room temperature showing a short magnetic range order. Radically, new approaches are needed to increase the intrinsic anisotropy that could lead to blocking temperatures much higher than the room temperature as well as novel collective behaviors when assembled into a material.

In the present work, we offer a possible alternative to enhancing magnetic anisotropy in nanoparticles and to generate a rare earth free permanent magnet via their assembly. Through wet chemical methods, we have synthesized a phase of transition metal carbides where the transition metal layers are far more separated than in pure bulk and embedded with intervening layers of the carbon atoms allowing only partial mixing between C and Co states. The separate layers result in large anisotropies, which are further compounded by the mixing with the carbon states, leading to materials with unusually large magnetocrystalline anisotropies. More specifically, we synthesize a biocompatible pure phase of cobalt carbide (Co_3C) nanomagnets with magnetic domains of size 8 nm that exhibit thermal and time stable long range ferromagnetic order up to 573 $\pm$ 2 K (the superparamagnetic limit), offering potential for novel magnetic materials. First principles theoretical investigations highlight the role of structure and composition on the observed behavior. Assemblies of the nanoparticles are found to behave as permanent magnets with magnetic characteristics that rival those of rare earth permanent magnets.

The magnetic behavior of the nanoparticles is best rationalized within a model of uniaxial anisotropy. The magnetic anisotropy energy (MAE) of the particle is proportional to $\sin^2\theta$, where θ is the angle between the magnetization and the easy axis. At absolute zero, the magnetization lies along one of two energy minima (θ equals 0° or 180°). When the temperature is raised above zero, the magnetization direction can fluctuate depending on the thermal energy k_BT and the energy barrier $K_{eff}V$ (K_{eff} is the effective crystalline anisotropy, and V is the particle volume), that exists at $\theta = \pm 90°$. Thus, given the ratio of the energy barrier to k_BT and knowing the resonant frequency, one can compute the average time between random reversals that are strongly dependent on the particle size and temperature. As an example, a factor of 2 change in the particle diameter can change the reversal time from 100 years to 100 nanoseconds.

In this study, the Co_3C particles were synthesized using polyol method described elsewhere[12] and were characterized using x-ray diffractometer to yield 100% of orthorombic-Co_3C nanomagnets (Figure 1). The x-ray diffraction (XRD) exhibits distinct peaks showing single phase Co_3C

a)Authors to whom correspondence should be addressed. Electronic addresses: aelgendy@vcu.edu; snkhanna@vcu.edu; and ecarpenter2@vcu.edu

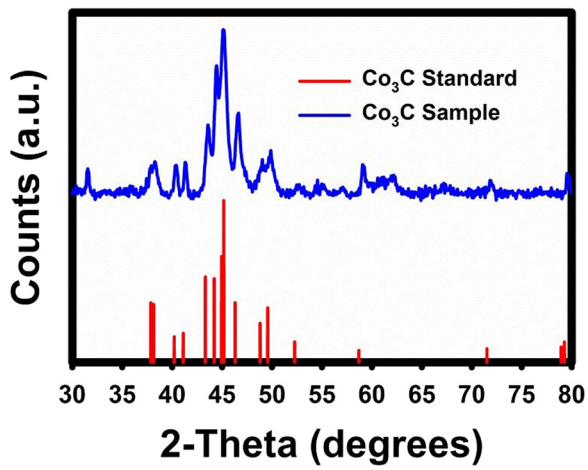

FIG. 1. XRD analysis for the synthesized Co_3C.

nanoparticles. The observed peak broadening reveals a smaller grain size of the particles which can be calculated using the well-known Sherrer equation to be around 11 ± 3 nm. The magnetization dependence on the external magnetic field was measured for the prepared sample at different temperatures ranging from 50 to 400 K (Figure 2(a)). The observed magnetization shows ferromagnetic behavior for the Co_3C nanomagnet and there is no knee observed behind the remanence magnetization M_r proving the formation of the pure phase carbides in agreement with the result from XRD. The Co_3C shows high coercivity (H_C) which increases with decreasing temperature.

The temperature dependent coercivity up to 650 K can be used to determine the blocking temperature by using relations that have been established before in Ref. 13. To this end, we have plotted the observed coercivity as a function of $T^{1/2}$ in Figure 2(b). The data reveal blocking temperature T_B at $H_C = 0$ to be 571 K and the coercivity H_{C0} at 0 K to be 9.5 kOe. From those results, the effective magnetocrystalline anisotropy K_{eff} and the particle size can be determined using Neel Brown equation[13] and magnetization dependence on domain size relation[11] to be $7.5 \pm 1.0 \times 10^5$ J/m^3 and 8.1 ± 0.5 nm, respectively. The magnetic domain size can be estimated from the magnetization studies by evaluating the initial slopes of the M(H) curves. Note that the major contribution to the initial slope arises from the largest magnetic domains. Their larger magnetization vectors are more easily oriented by the magnetic field, and thus, an upper limit to the magnetic domain size can be estimated. Further, within a single domain, the anisotropy is dominated by exchange interactions. Theoretical studies can help elucidate the origins of these interactions. The observed hysteresis curves were showing a decrease in the H_C till 600 K and an increase thereafter while the M_S was decreasing even after 600 K. Such a behavior indicates the presence of long range order and reveals a Curie temperature T_C of around 650 K, further indicating no change in the structure as a result of the high temperature measurement at 650 K.

To further ascertain the accuracy of the size, we performed the transmission electron microscope (TEM) measurements on the sample. The resulting images reveal a narrow distribution of rod nanoparticles with diameter around 10 ± 3 nm in good agreement with the magnetic domain size determined from the magnetic study (Figure 2(c)). A blocking temperature of 571 K and the effective anisotropy of $7.5 \pm 1.0 \times 10^5$ J/m^3 are both startling findings. This

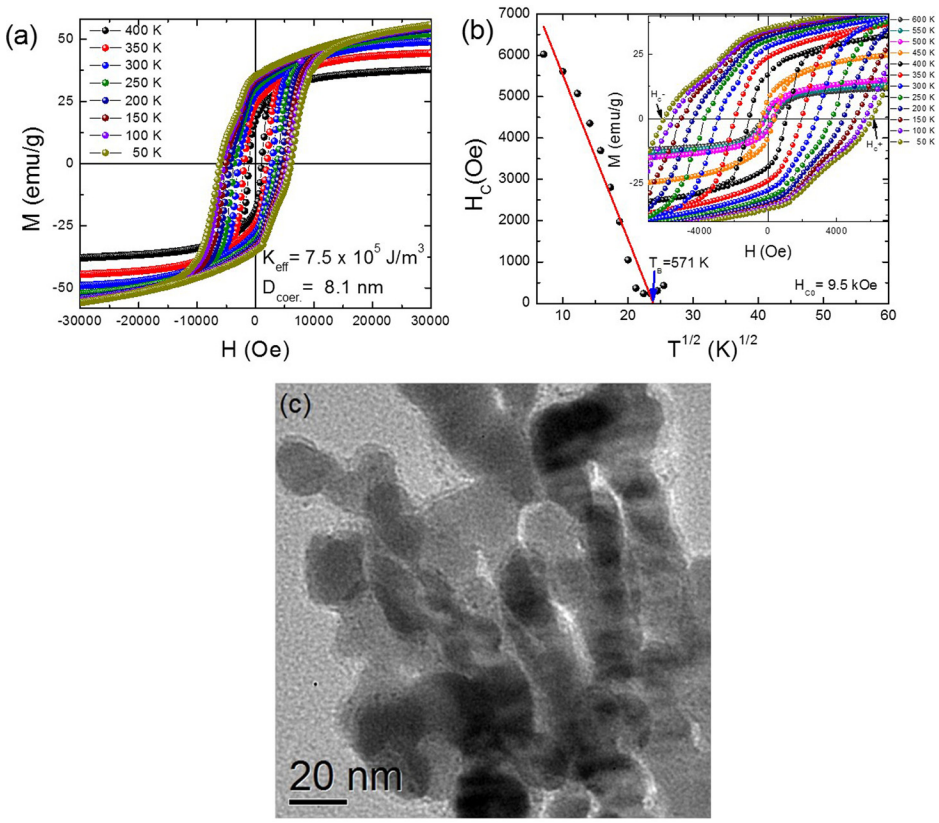

FIG. 2. Magnetic properties of the synthesized Co_3C. (a) The magnetic hysteresis loops at different temperatures. (b) The Coercivity dependence on temperature to determine T_B and H_{C0}. (c) TEM image for the Co_3C nanoparticles.

is particularly surprising since bulk Co is a soft magnetic material with a magnetic anisotropy of 4.1×10^5 J/m^3.[14] In particular, the anisotropy per Co atom in the carbide material is much larger than bulk Co since the carbide has less number of Co atoms per unit volume than pure Co. Further, carbon is known to quench the magnetic moment. The observed values are also much higher than previously reported values for particles of this size. As previously mentioned, it has recently been proposed that the blocking temperature of cobalt nanoparticles can be enhanced by coating the nanoparticles with an oxide layer. For example Skumryev *et al*. have reported synthesizing Co@CoO core-shell nanoparticles with a blocking temperature of 290 K.[9,10] These authors suggest that an exchange bias between the core and outside shell leads to the enhancement. However, the blocking temperatures in these studies are around the room temperature. In the present work, on the other hand, the blocking temperature tends to be much higher values by mixing soft magnetic material with a non-magnetic material. The results not only show nanoparticles with a larger T_B but that the current phase of Co_3C nanoparticles is stable up to 571 K.

In order to probe the microscopic origin of the observed large anisotropy, we undertook First principles density functional theory investigations.[15] Since the present phase consists of cobalt layers separated via carbon layers, we undertook investigations of the magneto crystalline anisotropy in this phase, which was calculated by determining the contribution from spin-orbit coupling to the total energy by constraining the magnetic moment along various directions characterized by the spherical angles θ and φ.[16,17] The total energy can then be divided into two parts, one is the direction-independent contribution, and the other is the small angular-dependent variation of energy. The second part determines the so-called anisotropy energy, which can be written down as follows:

$$\Delta E(\theta,\varphi) = E(0,0) + V\sin^2(\theta-\theta_0) \times \{K + K'\cos[2(\varphi-\varphi_0)]\}$$

Here K and K′ are two magnetic anisotropy constants of the nanoparticle, and the spherical angles θ_0 and φ_0 correspond to the easy axis directed along a minimum of anisotropy energy. In order to determine K and K′, we first carried out calculations of the $\Delta E(\theta,\varphi)$ by constraining moment along various directions, until a local minimum of the total energy is reached. For Co_3C, we found an easy axis along [001] direction with spherical angles $\theta_0 = \varphi_0 = 0°$ (Figure 3). As shown in Figure 3, the $\Delta E(\theta,\varphi)$ was calculated at different θ at constant $\varphi = 0°$ and $\varphi = 90°$. The above equation was then fitted to the calculated energies to determine the anisotropy constants. The calculated K and K' were 8.4×10^5 J/m^3 and -0.61×10^5 J/m^3, respectively. The fitting of the experimental data leads to an effective K_{eff} that does not involve variation over φ. Using the calculated constants, according to the above equation, the theoretical K_{eff} lies between two values, minimum (K + K′) 7.8×10^5 J/m^3 at $\varphi = 0°$ and maximum (K-K′) 9.0×10^5 J/m^3 at $\varphi = 90°$. The calculated values are in a good agreement with the experimental measurement of $7.4 \pm 1.0 \times 10^5$ J/m^3 noted above indicating that the primary contributor to the experimental anisotropy is the magneto-crystalline energy. Further studies were undertaken to identify the microscopic origin for the large values.

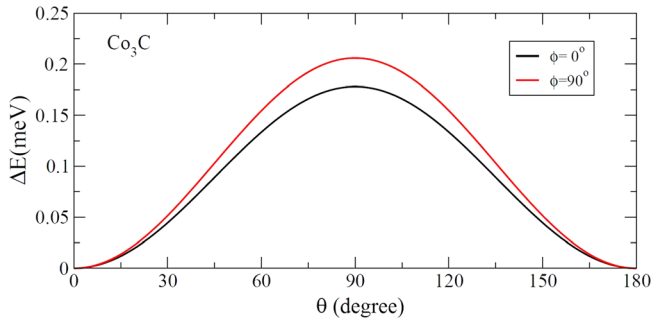

FIG. 3. Magnetic anisotropy energy $\Delta E(\theta,\varphi)$ at two angles $\varphi = 0°$ and $\varphi = 90°$.

In order to further quantify how such a mixing leads to an increase in MAE, we examined the band structure and the electronic states with large *d*-character in the carbide materials. The MAE in transition metal systems is small, and, as has been previously shown, a second order perturbation calculation of the spin orbit interaction can provide the microscopic picture.[16,17] Within the second order model, the MAE is determined by the matrix element of the spin orbit interaction between the occupied and the unoccupied states. We therefore proceeded to examine the location of the occupied and unoccupied Co *d*-states close to Fermi energy for the three interesting cases namely, pure bulk cobalt, structure of the nanoparticles with cobalt layers without the carbon layers, and the cobalt carbide with carbon layers. In Figure 1S of supplementary material,[20] we show the energy bands along Γ to X for the actual carbide material and for the separated cobalt layers alone. The states with larger d-component are shown by the dark dots. To further quantify the change in anisotropy, we examined the energy difference between the states at the Γ and X point for the nanostructures and the pure hexagonal cobalt (Table I). The separation into layers decreases the energy difference, thus increasing the anisotropy. The mixing with carbon further reduces this difference adding to the increase and resulting in giant anisotropic values. Similar enhancements in anisotropy through reduction of the separation between occupied and unoccupied states have been previously seen in other systems.[18]

For practical applications of the current nanoparticles, it is interesting to investigate the fluctuation time between two magnetization directions known as Neel-relaxation time (τ_N). It is related to the anisotropy energy via $\tau_N = \tau_0 e^{K_{eff}V/kBT}$. Using the anisotropy values, we determined it as a function of temperature, and the results are shown in Figure 4. The inset shows the two minima of the anisotropy energy at $\theta = 0°$ and 180° while the maximum anisotropy

TABLE I. MAE of bulk Co_3C and Co_3E (E = empty sphere) in units of meV per formula. The zero energy is set as the reference, and the corresponding direction is the easy axis.

	[100]	[010]	[001]	[110]	[111]
Co_3C	0.178	0.206	0	0.191	0.128
Co_3E	0.109	0.016	0	0.062	0.042

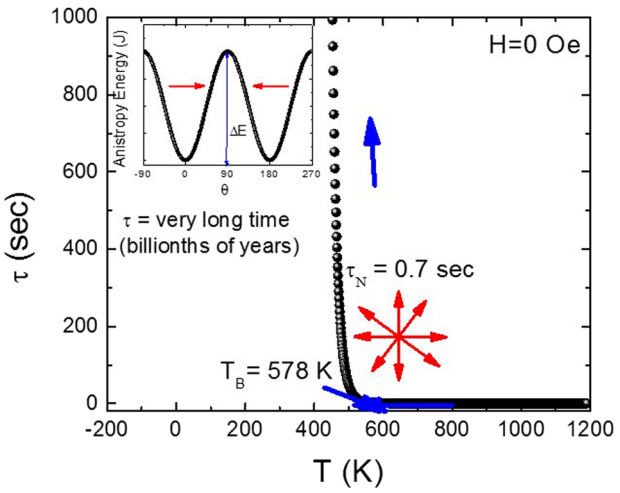

FIG. 4. The fluctuation time dependence on temperature, inset plot is showing the two minima of the E_{anis} and the maximum value at $\theta = 90°$.

energy occurs when the magnetic moment is 90° to the easy axis. As shown in Figure 4, at low temperature where the thermal energy is very small compared to the anisotropy energy, the fluctuation time between two directions is very long (10^9 years) revealing thermally stable magnetic order. Then by increasing the temperature, the fluctuation time stays longer till the temperature is close to 300 K, the time drops to 434 years (thermal stable magnetic order). Upon further raising the temperature close to T_B at 571 K, the fluctuation time drops to 0.7 s, and the magnetic moments fluctuate freely. As mentioned earlier, this occurs due to the increase of the thermal energy that becomes larger than the anisotropy energy. The magnetic order is then not thermally stable, and superparamagnetic (SPM) behavior dominates. We can also use the observed anisotropy to determine the rate of change of the magnetic moment direction ($d\theta/dt$) as a function of temperature using the expression $25\,k_BT = K_{eff}V\,Sin^2\,\theta$. The results are shown in Figure 5(a). From these, the T_B and the Curie temperature T_C (threshold between SPM and paramagnetic behavior) are determined to be 577 K and 641 K, which is in a good agreement with the value determined from the H_C dependence of Temperature (Figure 2(b)). At low temperature, $K_{eff}V > k_BT$, and the $d\theta/dt$ is very small indicating that the magnetic moment takes a long time to fluctuate from one direction to another direction. Once the temperature is close to T_B, the thermal energy is comparable to the anisotropy energy $K_{eff}V \approx k_BT$ and $d\theta/dt$ increases till it reaches the maximum value, and the superparamagnetic behavior dominates. Further increase in the temperature beyond T_B results in a decrease of the $d\theta/dt$ that becomes very small close to T_C at 641 K. Once T_C has been reached, the temperature effect on $d\theta/dt$ is negligible, and the magnetic moments take random directions and behave as paramagnetic. On the other hand, information regarding the shape of the particles can be determined from the T_C dependence on particle size by applying cohesive energy model to our material (Figure 5(b)).[6] As seen from the plot, T_C exhibits a linear relation with the number of atoms that is directly proportional to the particle size for 3 different shapes, such as sphere, cube, and cylinder. By comparing our result to the plot, we have found that our experimentally obtained T_C lies in the range of cylindrical shaped nanoparticles which is consistent with our TEM image. Also by comparing our particle size result to the plot, we have found that the calculated T_C is around 645 K, which is in a good agreement with our experimental result based on M × H measurements.

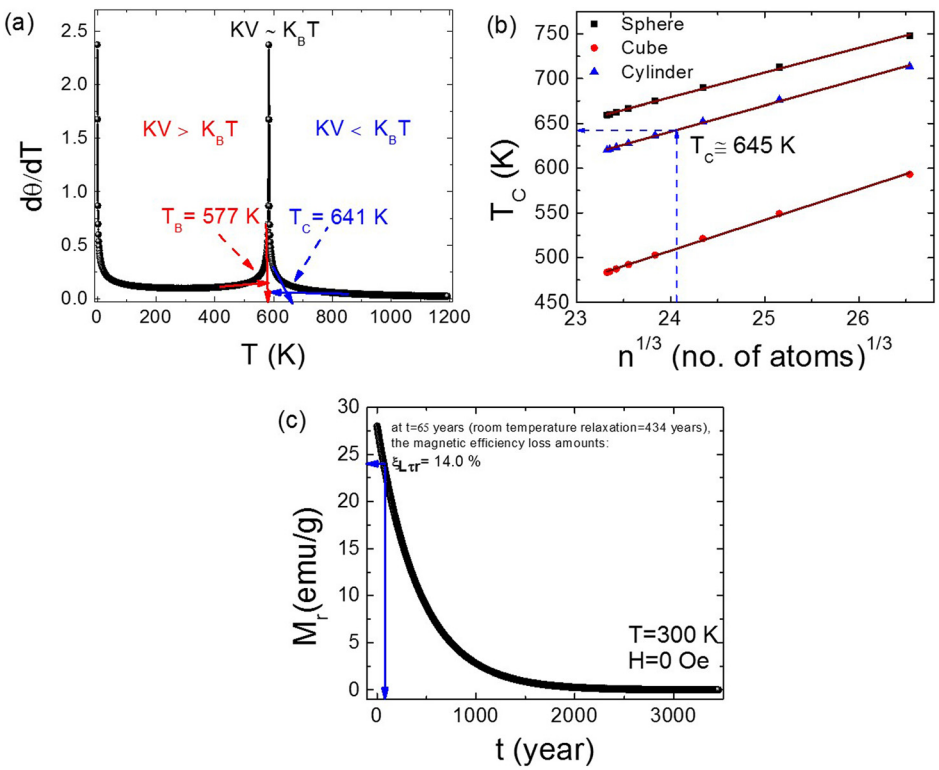

FIG. 5. Magnetic properties of the synthesized Co_3C. (a) The temperature dependence of $d\theta/dt$. (b) T_C dependence on No. of atoms for different shapes. (c) The remnant magnetization dependence on temperature revealing information regarding the magnetic efficiency loss.

In order to use the Co_3C nanomagnets for data storage applications, we also determined the magnetic efficiency loss. Figure 5(c) shows the remnant magnetization (M_r) dependence on time at zero magnetic fields and room temperature. The magnetic efficiency loss (ζ) at room temperature amounts to around 14% after 65 years of using the materials. This result opens a door for a new material for applications in the data storage technology.

The above findings on the effect of the temperature and the particle size on the direction and the fluctuation time of the magnetic moment could be condensed into a single simple 3D figure that represents the effect of temperature on the rotation of the magnetic moment. This is shown in Figure 2S (see supplementary material[20]). The color indicates the change in the temperature range starting from the lower temperatures (blue regions) up to the very high temperatures (black regions). The effect of the thermal energy on change of the magnetic moment direction has been implied from 0° to 135° resulting in a magnetic moment rotation image of the particle around its easy axis (Figure 2S).

To conclude, the present studies indicate that unusually large MAE can be accomplished in cobalt carbide nanoparticles consisting of cobalt layers separated by carbon atoms. The increased anisotropy is mainly driven by spin orbit coupling. The separation into layers increases the anisotropy, and the effect is enhanced by the intervening carbon layers. The carbon *p*-states partially mix with Co *d*-states to reduce the separation between the occupied and unoccupied *d*-states, leading to the large MAE, a superparamagnetic blocking temperature in excess of 571 K, and a higher H_C and K_{eff}, even for particles with size less than 10 nm. The current nanoparticles could be used for a new generation of thermal stable data storage devices and when assembled, form strong permanent magnets. Since the separation between occupied and unoccupied states is sensitive to the composition and the underlying atomic structure, the present work opens the possibility of further enhancing the MAE through control of the composition and the size of the particles.[19] Towards this end, it will be interesting to examine if other transition metal carbides could also exhibit similar enhancements.

All authors would like to acknowledge the help of the Virginia Commonwealth Nanomaterials Core Characterization Facility. A.A.E., M.Q., Z.J.H., and E.E.C. acknowledge financial support from ARPA-e REACT project No. 1574-1674. S.N.K. acknowledges support from U.S. Department of Energy (DOE) through Grant No. DE-FG02-11ER16213.

[1]H. Kuramochi, H. Akinaga, Y. Semba, M. Kijima, T. Uzumaki, M. Yasutake, A. Tanaka, and H. Yokoyama, Jpn. J. Appl. Phys., Part 1 **44**, 2077 (2005).
[2]A. A. El-Gendy, E. M. M. Ibrahim, V. O. Khavrus, Y. Krupskaya, S. Hampel, A. Leonhardt, B. Büchner, and R. Klingeler, Carbon **47**, 2821 (2009).
[3]H. Wang, S. P. Wong, W. Y. Cheung, N. Ke, M. F. Chiah, H. Liu, and X. X. Zhang, J. Appl. Phys. **88**, 2063 (2000).
[4]J. J. Delaunay, T. Hayashi, M. Tomita, S. Hirono, and S. Umemura, Appl. Phys. Lett. **71**, 3427 (1997).
[5]M. Johannsen, U. Gneveckow, K. Taymoorian, B. Thiesen, N. Waldöfner, R. Scholz, K. Jung, A. Jordan, P. Wust, and S. A. Loening, Int. J. Hyperthermia **23**, 315 (2007).
[6]A. A. El-Gendy, T. Almugaiteeb, and E. E. Carpenter, J. Magn. Magn. Mater. **348**, 136 (2013).
[7]S. N. Khanna and S. Linderoth, Phys. Rev. Lett. **67**, 742 (1991).
[8]D. Weller and A. Moser, IEEE Trans. Magn. **35**, 4423 (1999).
[9]V. Skumryev, S. Stoyanov, Y. Zhang, G. Hadjipanayis, D. Givord, and J. Nogués, Nature **423**, 850 (2003).
[10]J. Eisenmenger and I. K. Schuller, Nature Mater. **2**, 437 (2003).
[11]A. A. El-Gendy, V. O. Khavrus, S. Hampel, A. Leonhardt, B. Buechner, and R. Klingeler. J. Phys. Chem. C **114**, 10745 (2010).
[12]K. J. Carroll, Z. J. Huba, S. R. Spurgeon, M. Qian, S. N. Khanna, D. M. Hudgins, M. L. Taheri, and E. E. Carpenter, Appl. Phys. Lett. **101**, 012409 (2012).
[13]E. C. Stoner and E. P. Wolfarth, Philos. Trans. R. Soc. London, Ser. A **240**, 599 (1948).
[14]W. Sucksmith and J. E. Thomson, Proc. R. Soc. London, Ser. A **225**, 362 (1954).
[15]Vienna *ab initio* Simulation Package (VASP) is using the projector-augmented wave pseudopotentials, and the valence states of Co and C were described by [Ar] $3d^8 4s^1$ and [He] $2s^2 2p^2$ electron configurations, respectively. The exchange correlation contributions were incorporated using generalized gradient functional proposed by Perdew, Burke, and Ernzerof in a GGA+U approach with a U value of 4.0 eV. A plane wave basis with an energy cutoff of 400 eV and a Mokhorst-Pack scheme of $9 \times 9 \times 9$ division are taken. Co_3C has an orthorhombic crystal structure with experimental lattice constant a = 5.016 Å, b = 6.730 Å, and c = 4.445 Å, which is fully relaxed till the forces on all atoms are less than 0.01 eV/Å. G. Kresse and J. Furthmuller, Phys. Rev. B **54**, 11169 (1996); G. Kresse and J. Hafner, J. Phys. Condens. Matter **6**, 8245 (1994); S. L. Dudarev, G. A. Botton, S. Y. Savrasov, C. J. Humphreys, and A. P. Sutton, Phys. Rev. B **57**, 1505 (1998).
[16]E. I. Kondorskii and E. Straube, Sov. Phys. JETP **36**, 188 (1973).
[17]M. R. Pederson and S. N. Khanna, Phys. Rev. B **60**, 9566 (1999).
[18]T. Burkert, L. Nordstrom, O. Eriksson, and O. Heinonen, Phys. Rev. Lett. **93**, 027203 (2004).
[19]J. Kortus, T. Baruah, M. R. Pederson, C. Ashman, and S. N. Khanna, Appl. Phys. Lett. **80**, 4193 (2002).
[20]See supplementary material at http://dx.doi.org/10.1063/1.4862260 for detailed description of the thermal energy effect on direction of magnetic moment and the band structures.